



# Microstructure and chemical analysis of four calcium silicate-based cements in different environmental conditions

K. Ashofteh Yazdi<sup>1</sup> · Sh. Ghabraei<sup>1</sup> · B. Bolhari<sup>1</sup> · M. Kafili<sup>2</sup> · N. Meraji<sup>1</sup>  · M. H. Nekoofar<sup>1,3</sup> · P. M. H. Dummer<sup>3</sup>

Received: 12 June 2017 / Accepted: 15 February 2018 / Published online: 30 March 2018  
© Springer-Verlag GmbH Germany, part of Springer Nature 2018

## Abstract

**Objective** The objective of this study was to analyze the microstructure and crystalline structures of ProRoot MTA, Biodentine, CEM Cement, and Retro MTA when exposed to phosphate-buffered saline, butyric acid, and blood.

**Methods and materials** Mixed samples of ProRoot MTA, Biodentine, CEM Cement, and Retro MTA were exposed to either phosphate-buffered saline, butyric acid, or blood. Scanning electron microscope (SEM) and [energy-dispersive X-ray spectroscopic](#) (EDX) evaluations were conducted of specimens. X-ray diffraction (XRD) analysis was also performed for both hydrated and powder forms of evaluated calcium silicate cements.

**Results** The peak of tricalcium silicate and dicalcium silicate detected in all hydrated cements was smaller than that seen in their unhydrated powders. The peak of calcium hydroxide (Ca(OH)<sub>2</sub>) in blood- and acid-exposed ProRoot MTA, CEM Cement, and Retro MTA specimens were smaller than that of specimens exposed to PBS. The peak of Ca(OH)<sub>2</sub> seen in Biodentine™ specimens exposed to blood was similar to that of PBS-exposed specimens. On the other hand, those exposed to acid exhibited smaller peaks of Ca(OH)<sub>2</sub>.

**Conclusion** Exposure to blood or acidic pH decreased Ca(OH)<sub>2</sub> crystalline formation in ProRoot MTA, CEM Cement and Retro MTA. However, a decrease in Ca(OH)<sub>2</sub> was only seen when Biodentine™ exposed to acid.

**Clinical relevance** The formation of Ca(OH)<sub>2</sub> which influences the biological properties of calcium silicate cements was impaired by blood and acid exposures in ProRoot MTA, CEM Cement, and Retro MTA; however, in the case of Biodentine, only exposure to acid had this detrimental effect.

**Keywords** Biodentine · Calcium silicate cement · CEM cement · EDX · MTA · SEM · XRD

---

**Electronic supplementary material** The online version of this article (<https://doi.org/10.1007/s00784-018-2394-1>) contains supplementary material, which is available to authorized users.

---

✉ N. Meraji  
meraji\_n@yahoo.com

✉ M. H. Nekoofar  
nekoofar@tums.ac.ir; nekoofarmh@cardiff.ac.uk

<sup>1</sup> Department of Endodontics, School of Dentistry, Tehran University of Medical Sciences, Tehran, Iran

<sup>2</sup> Department of Endodontics, School of Dentistry, Tabriz University of Medical Sciences, Tabriz, Iran

<sup>3</sup> School of Dentistry, College of Biomedical and Life Sciences, Cardiff University, Cardiff, UK

## Introduction

Calcium silicate cements (CSCs) have various indications of use in endodontics and their potential clinical applications have increased over the years. Mineral trioxide aggregate (MTA) was the first CSC introduced in endodontics. Although having a variety of favorable properties, this CSC has several disadvantages such as difficult handling properties and induction of tooth discoloration [1–4]. Recently, a variety of CSCs have been introduced to overcome these disadvantages.

Biodentine was introduced as a fast setting dentine replacement material [5] with high compressive strength [6, 7]. It is composed of tricalcium silicate, zirconium oxide, and calcium carbonate, which when mixed with its liquid containing calcium chloride and a water-soluble polymer, sets rapidly [8]

and forms calcium hydroxide ( $\text{Ca}(\text{OH})_2$ ) as a by-product of hydration [9].

Calcium-enriched mixture (CEM) Cement was introduced as a white CSC claiming to have no discoloration potential [10–12]. It is composed of  $\text{CaO}$  (51.75%),  $\text{SO}_3$  (9.53%),  $\text{P}_2\text{O}_5$  (8.49%),  $\text{SiO}_2$  (6.32%), and minor components of  $\text{Al}_2\text{O}_3$ ,  $\text{Na}_2\text{O}$ ,  $\text{MgO}$ , and  $\text{Cl}$  [13].

Retro MTA is another fast setting CSC and is said to have less discoloration potential [14]. It consists of calcium carbonate, silicon dioxide, aluminum oxide, and calcium zirconia [15].

The clinical applications of MTA have been suggested for all aforementioned CSCs [5, 16, 17]. In most clinical applications related to the field of endodontics such as root end filling, perforation sealing, vital pulp therapy, and regeneration, CSCs encounter blood and/or in infectious conditions, acidic pH. This contact occurs when these cements are undergoing hydration and maturation [1]. Therefore, knowledge of the effect of these environmental conditions on the chemical compounds and hydration process of these cements is of clinical significance. Some studies have shown that exposure to these conditions affect some properties in different cements [18–20] such as their setting, expansion and physical properties [21]. But data on the effect of different conditions on the properties of Retro MTA and CEM Cement are limited.

The aim of this study was to evaluate the effect of exposure to butyric acid, a metabolism by-products of anaerobic bacteria dominant in endodontic infections and the most common fatty acid found in infectious conditions with endodontic origin [22], and blood during setting on the chemical compounds and hydration process of ProRoot MTA, Biodentine, CEM Cement, and Retro MTA. The null hypothesis was that exposure to blood and acid will not affect these CSCs.

## Methods and materials

Plexiglass molds with an internal diameter of 4 and 6 mm heights were fabricated by CNC laser cutting.

Four CSCs were evaluated (Table 1):

1. ProRoot MTA (Dentsply Sirona, Ballaigues, Switzerland)
2. Biodentine (Septodont, Saint Maur des Fosses, France)
3. CEM Cement (Bionique, Tehran, Iran)
4. Retro MTA (BioMTA, Seoul, Republic of Korea)

Three exposure conditions were evaluated:

- a. Phosphate-buffered saline (PBS) (pH = 7.4) (Merck, Darmstadt, Germany)
- b. Whole human blood (WHB)
- c. Butyric acid (BA)(pH = 5.4) (Merck, Darmstadt, Germany)

For preparation of ProRoot MTA and CEM Cement slurries, 1 g of their powder was placed in an empty, clean plastic capsule, and 0.33 mL of the respective liquid was added [23]. For Retro MTA, the powder content of one pack was placed in the same type of plastic capsule and three drops of its liquid were added as suggested by the manufacturer. Biodentine powder is delivered in a capsule, and its liquid is supplied in a single-dose container. Each capsule was mixed with five drops of its liquid. The encapsulated materials were then mechanically mixed for 30 s at 4500 rpm [18] using an amalgamator (Silamat; IvoclarVivadent AG, Liechtenstein).

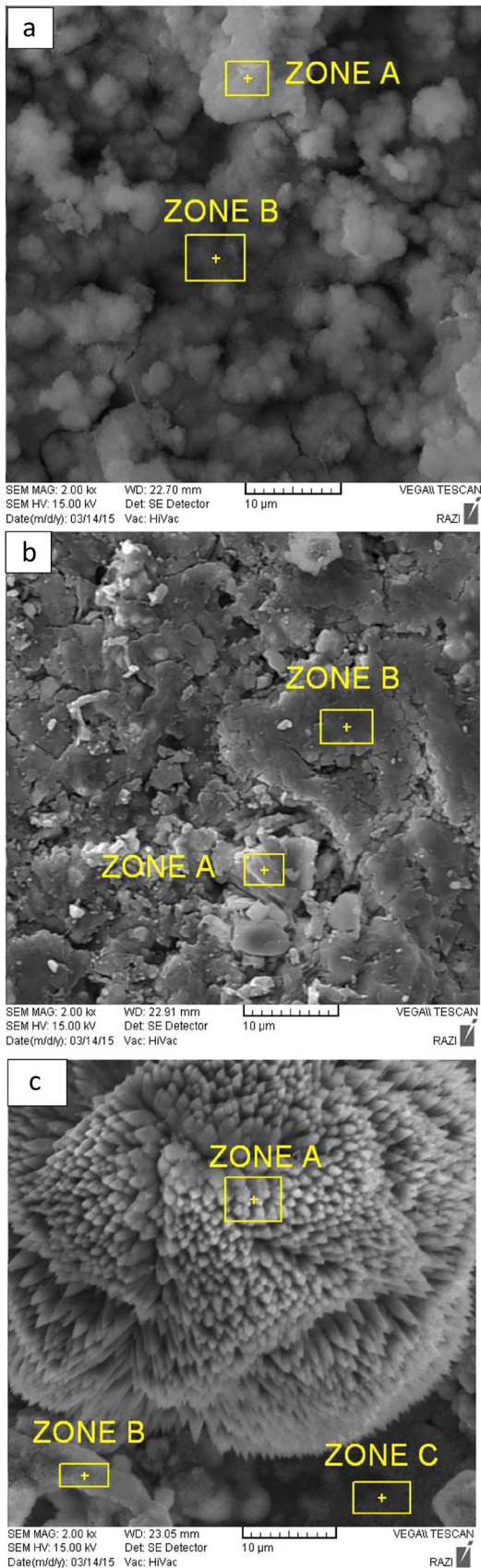
Prior to slurry placement, each mold was filled with either PBS, WHB or BA according to the specific subgroup and excess liquid was aspirated after 20 s. The molds were then filled with the prepared cements using minimal pressure. The materials were then subjected to ultrasonic energy for 30 s at a power scale of 5 using a BUC-1 Spartan tip (Obtura Spartan, Fenton, MO, USA) attached to a Suprasson\_P5 Booster (Satelec, Merignac, France) [18, 23]. After initial setting, specimens were placed in Eppendorf tubes containing the respective exposure liquid: PBS, WHB, or BA. Placement was in a way that the lower surface of each specimen would be in contact with the liquid. A moist cotton pellet was then placed over the specimens. They were incubated for 7 days in 37 °C and fully saturated conditions.

After the incubation period, the surface in contact with either PBS, WHB, or BA was coated with gold and analyzed with a scanning electron microscope (SEM) equipped with EDX (SEM-EDX 515, Phillips, Eindhoven, the Netherlands). Images with  $\times 400$  and  $\times 2000$  magnifications were considered adequate for the characterization of the microstructure. Element analysis was performed on selected segments with crystalline and amorphous structure.

Both hydrated (mixed) and unhydrated (powder) cements were mounted for XRD analysis. The hydrated cements were milled into a fine powder. An automated X-ray diffractometer (X'Pert PRO MPD, Philips) with  $\text{Cu K}\alpha$  radiation was set at 40 kVp and 30 mA. Data were collected from scan range of 15–55 with a step size of  $0.02^\circ$ . X'Pert High score plus software (Spectrum Viewer Basic 2.6.3, PANalytical, Nottingham, UK) was used for the analysis. The peaks of each sample were matched with those of the International Center for Diffraction Data (ICDD) database (International Center for Diffraction Data, Newton Square, PA, USA). By comparing the size of each peak representing a crystalline phase between groups, their relative amounts were estimated.

## Results

The results of SEM and EDX evaluations of the CSCs exposed to the various media are shown in Figs. 1, 2, 3, and 4.

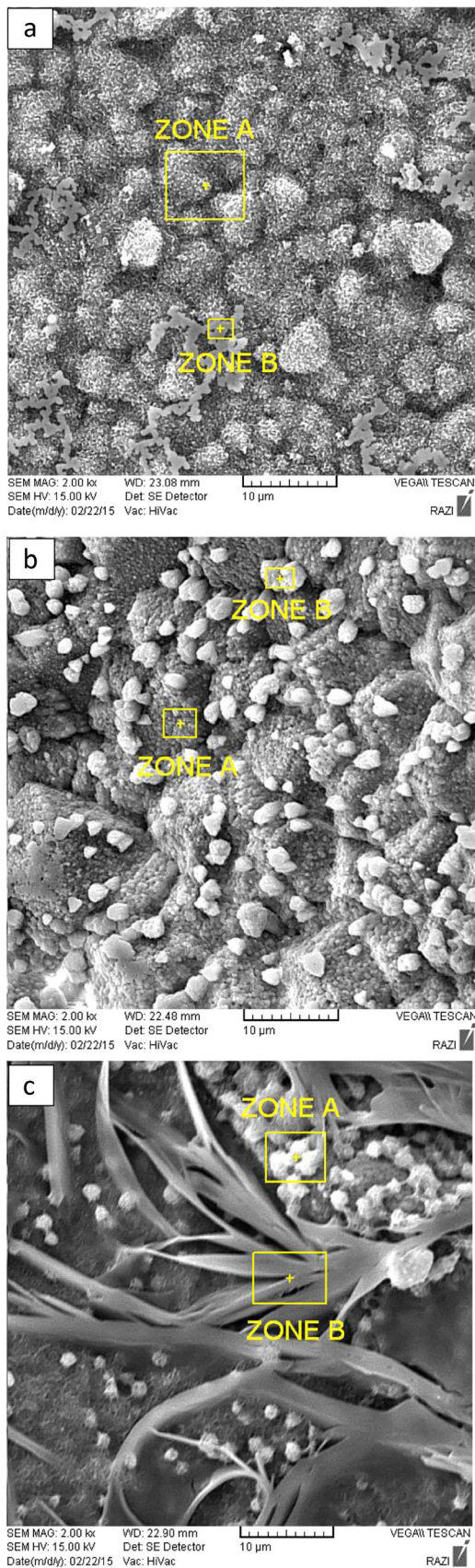


Element	Wt% in different zones	
	A	B
Carbon	9.38	7.24
Oxygen	45.17	38.03
Calcium	31.53	36.84
Bismuth	4.61	8.23
Silicon	8.78	9.58
Aluminum	0.51	-
Trace elements	0.02	0.08

Element	Wt% in different zones	
	A	B
Carbon	11.54	16.50
Oxygen	42.96	39.81
Calcium	32.77	29.13
Bismuth	11.58	9.59
Iron	0.17	0.71
Silicon	0.43	3.28
Aluminium	0.22	0.48
Trace elements	0.33	0.5

Element	Wt% in different zones		
	A	B	C
Carbon	10.80	6.09	9.64
Oxygen	45.17	37.82	44.76
Calcium	40.20	46.86	38.10
Bismuth	3.59	4.77	2.91
Silicon	-	4.40	4.20
Trace elements	0.24	0.06	0.39

**Fig. 1** Scanning electron microscopic (SEM) images and EDX results of ProRoot MTA exposed to (a) PBS, (b) blood, and (c) butyric acid showing globular crystalline structures in the PBS and blood exposed specimens and prismatic crystalline structures in those exposed to butyric acid

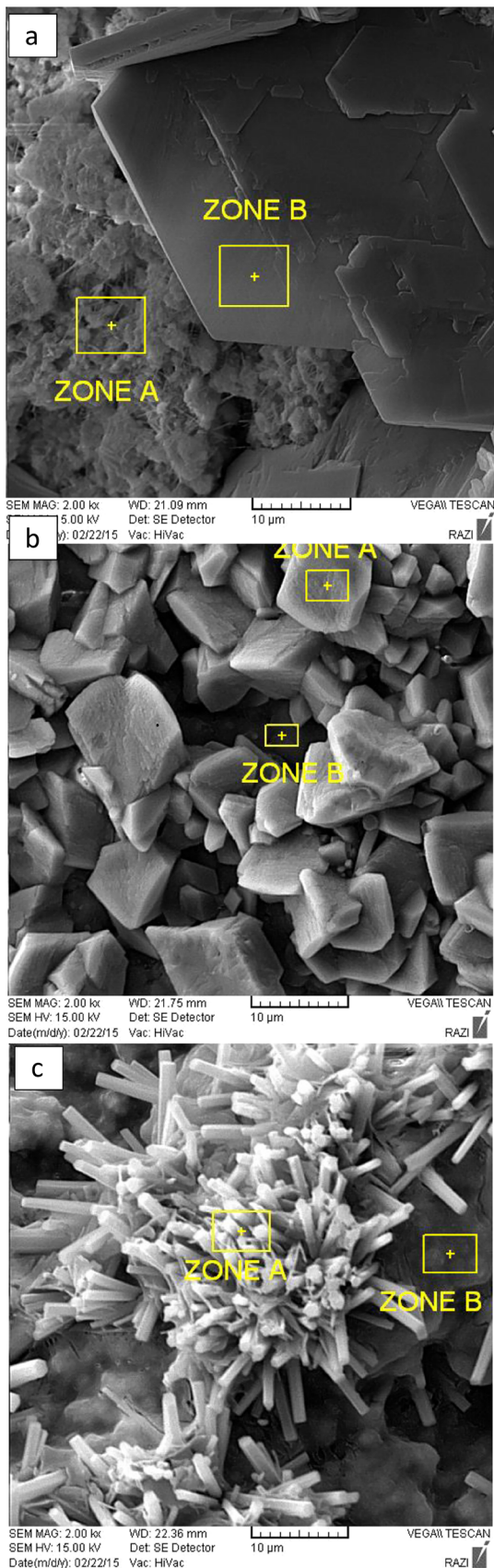


Element	Wt% in different zones	
	A	B
Carbon	5.34	5.99
Oxygen	37.69	39.79
Calcium	31.59	31.18
Zirconium	12.36	10.78
Chlorine	1.00	0.73
Silicon	9.72	8.95
Sodium	1.61	1.66
Trace elements	0.69	0.92

Element	Wt% in different zones	
	A	B
Carbon	9.16	11.81
Oxygen	26.13	36.94
Calcium	51.80	33.12
Zirconium	10.56	13.42
Chlorine	1.86	2.89
Silicon	-	0.87
Iron	-	0.54
Trace elements	0.49	0.41

Element	Wt% in different zones	
	A	B
Carbon	9.31	23.21
Oxygen	38.67	35.31
Calcium	40.07	32.44
Zirconium	9.10	6.59
Chlorine	1.26	0.53
Silicon	1.57	1.48
Trace elements	0.02	0.44

**Fig. 2** Scanning electron microscopic (SEM) images and EDX results of Biodentine exposed to (a) PBS, (b) blood, and (c) butyric acid showing globular crystalline structures in all exposure conditions

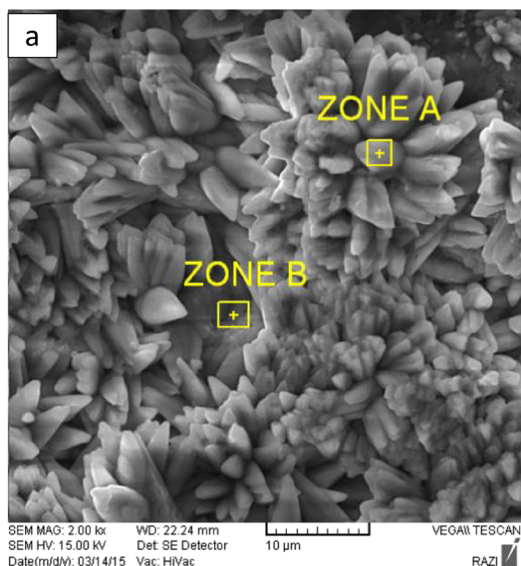


Element	Wt% in different zones	
	A	B
Carbon	-	1.41
Oxygen	26.58	41.43
Calcium	44.88	51.73
Silicon	1.86	-
Sulfur	4.74	0.92
Phosphorus	4.67	2.78
Zinc	4.73	-
Barium	12.14	1.38
Trace elements	0.4	0.35

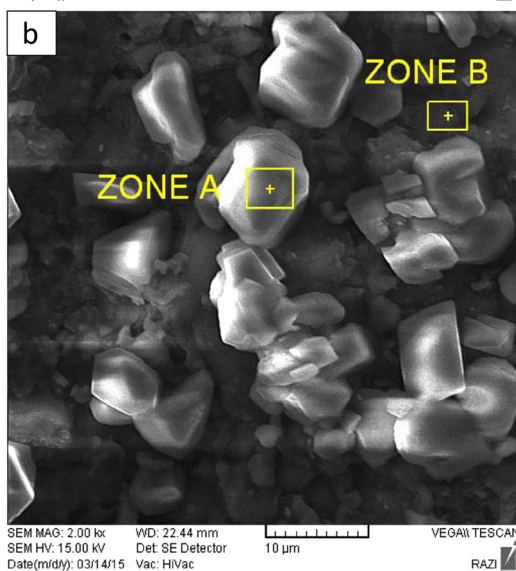
Element	Wt% in different zones	
	A	B
Carbon	10.50	0.50
Oxygen	41.39	8.46
Calcium	40.17	87.69
Sulfur	2.03	0.87
Phosphorus	5.49	0.88
Barium	-	1.60
Trace elements	0.42	-

Element	Wt% in different zones	
	A	B
Carbon	12.46	8.55
Oxygen	37.26	41.75
Calcium	27.43	33.02
Silicon	1.49	4.19
Sodium	0.44	2.65
Aluminium	4.14	0.67
Sulfur	3.14	-
Iron	0.76	-
Barium	12.49	-
Trace elements	0.39	9.17

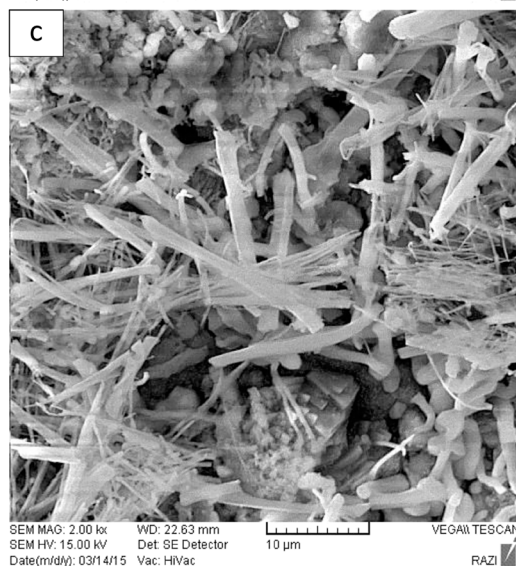
**Fig. 3** Scanning electron microscopic (SEM) images and EDX results of CEM Cement exposed to (a) PBS, (b) blood, and (c) butyric acid showing hexagonal, cubical, and needle-like crystalline structures in specimens exposed to PBS, blood, and butyric acid, respectively



Element	Wt% in different zones	
	A	B
Carbon	11.86	8.72
Oxygen	46.93	43.07
Calcium	40.00	47.81
Barium	0.78	-
Trace elements	0.43	0.4



Element	Wt% in different zones	
	A	B
Carbon	9.09	13.25
Oxygen	44.48	37.58
Calcium	45.81	48.10
Barium	0.60	1.06
Trace elements	0.02	0.01



Element	Wt% in different zones	
	A	B
Carbon	10.31	6.46
Oxygen	46.61	42.60
Calcium	41.07	45.70
Barium	0.89	-
Aluminum	0.80	0.55
Silicon	-	4.67
Trace elements	0.32	0.02

**Fig. 4** Scanning electron microscopic (SEM) images and EDX results of Retro MTA exposed to (a) PBS, (b) blood, and (c) butyric acid exhibiting prismatic, cubical, and needle-like crystalline structures in specimens exposed to PBS, blood, and butyric acid, respectively

**Table 1** CSCs evaluated

Cement	Composition		Manufacturer
	Powder	Liquid	
ProRoot MTA	Tricalcium silicate, tricalcium aluminate, dicalcium silicate, bismuth oxide	Distilled water	Dentsply Sirona, Ballaigues, Switzerland
Biodentine	Tricalcium silicate, zirconium oxide, calcium carbonate	Calcium chloride, a water-soluble polymer	Septodont, Saint Maur des Fosses, France
CEM Cement	Calcium oxide, sulfur trioxide, phosphorous Pentoxide, silicon dioxide, aluminum trioxide, sodium oxide, magnesium oxide, chloride	Water-based liquid	Bionique, Tehran, Iran
Retro MTA	Calcium carbonate, silicon dioxide, aluminum oxide, calcium zirconia complex	Distilled water	BioMTA, Seoul, Republic of Korea

SEM images of ProRoot MTA specimens exposed to PBS and blood revealed the presence of globular crystalline structures which disappeared in those exposed to butyric acid. Instead, prismatic crystalline structures were seen on the surface of those exposed to butyric acid (Fig. 1). EDX evaluations revealed the addition of Fe in the composition of crystalline structures in specimens exposed to blood.

Biodentine specimens contained globular crystalline structures on their surface in all exposure conditions (Fig. 2). EDX evaluations revealed the presence of Fe in the composition of the crystalline structures of specimens exposed to blood while the amorphous phase in these specimens lacked both Fe and Si.

CEM Cement revealed hexagonal, cubical, and needle-like crystalline structures in specimens exposed to PBS, blood, and butyric acid, respectively (Fig. 3). EDX evaluations revealed the presence of P in both crystalline and amorphous structures in specimens exposed to PBS and blood whereas this element was not detectable in those exposed to butyric acid. BA was also detected in all specimens regardless of the exposure conditions.

Retro MTA exhibited prismatic, cubical, and needle-like crystalline structures in specimens exposed to PBS, blood, and butyric acid, respectively (Fig. 4). EDX evaluations revealed the presence BA in all specimens regardless of the exposure conditions.

XRD evaluation of ProRoot MTA exposed to different media revealed the presence of tricalcium silicate and dicalcium silicate, alpha bismuth oxide, and  $\text{Ca}(\text{OH})_2$  in all specimens. The peak of tricalcium silicate and dicalcium silicate was smaller than that of unhydrated powder. The peaks of  $\text{Ca}(\text{OH})_2$  on blood- and acid-exposed specimens were smaller than that of specimens exposed to PBS. The unhydrated powder did not contain  $\text{Ca}(\text{OH})_2$  (Fig. 5).

All Biodentine specimens exposed to different media contained tricalcium silicate and dicalcium silicate, calcium carbonate, zirconium oxide, and  $\text{Ca}(\text{OH})_2$ . The peak of tricalcium silicate and dicalcium silicate was smaller than that seen in the unhydrated powder. The peak of tricalcium silicate

and dicalcium silicate and  $\text{Ca}(\text{OH})_2$  seen in specimens exposed to blood were similar to that of PBS-exposed specimens. On the other hand, those exposed to acid exhibited smaller peaks of  $\text{Ca}(\text{OH})_2$ . The acid-exposed specimens were also associated with smaller peaks of tricalcium silicate and dicalcium silicate in comparison to the blood-exposed specimens (Fig. 5).

XRD evaluation of CEM Cement exposed to the various media revealed the presence of tricalcium silicate and dicalcium silicate, calcium carbonate, barium sulfate, and  $\text{Ca}(\text{OH})_2$  in all specimens. The peak of tricalcium silicate and dicalcium silicate was smaller than that seen in unhydrated powder. The peak of  $\text{Ca}(\text{OH})_2$  on specimens exposed to blood and acid was smaller than when exposed to PBS (Fig. 5).

XRD evaluation of Retro MTA exposed to the media revealed the presence of tricalcium silicate, zirconium oxide, and  $\text{Ca}(\text{OH})_2$  in all specimens. The peak of tricalcium silicate was smaller than that seen in unhydrated powder. The peak of  $\text{Ca}(\text{OH})_2$  seen on specimens exposed to blood and acid was smaller than those exposed to PBS (Fig. 5).

## Discussion

In this study, three exposure conditions were evaluated: exposure to PBS (pH = 7.4), WHB, and BA (pH = 5.4). BA is a short-chain fatty acids produced by endodontic pathogens and the most common fatty acid found in endodontic infectious conditions [22]. It is usually used to reproduce acidic conditions in vitro [19, 24]. PBS is a simulated tissue fluid containing phosphate [25] that can be used for the purpose of mimicking normal in vivo conditions in laboratory studies [19, 26].

Scanning electron microscopy and EDX analysis together with X-ray diffraction analysis were used to assess the effect of exposure to several potential clinically relevant

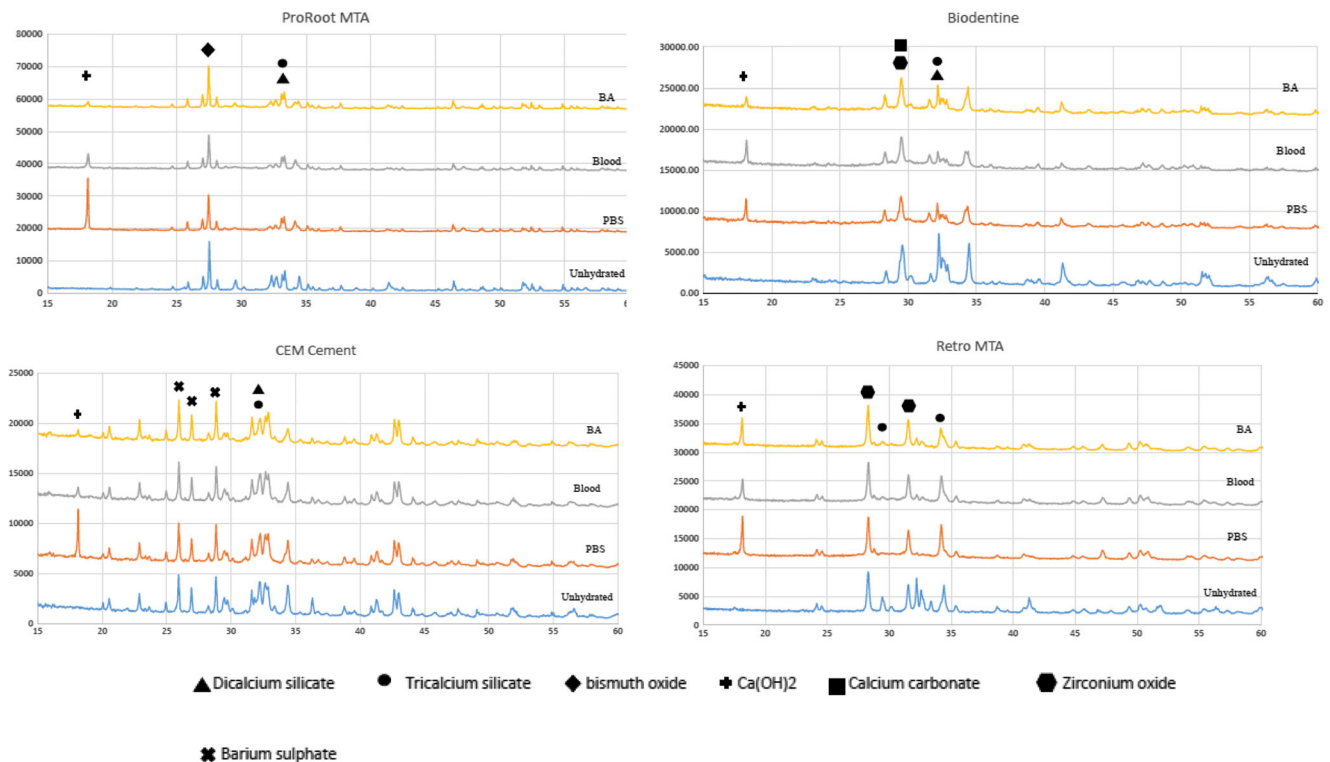


**Fig. 5** X-ray diffraction result of different experimental groups

environmental conditions on the composition and hydration process of various CSCs.

XRD is useful for identifying the crystalline phases of specimens. The intensity of each peak representative of a crystalline phase in XRD is proportional to the phase concentration [27]. However, a disadvantage of this analysis for CSCs is the superimposition of the peaks and the presence of multiple compounds within the materials [27]. An example of this superimposition is observed at  $52^\circ 2\theta$  for dicalcium silicate and tricalcium silicate crystalline structures as seen in Fig. 5. It should be noted that superimposition is also observed at  $25.8^\circ 2\theta$  for hydroxyapatite and barium sulfate making them indistinguishable.

Reduction in the peak size of tricalcium silicate and dicalcium silicate peaks and detection of  $\text{Ca}(\text{OH})_2$  in the hydrated forms of all the CSCs in comparison with their powder counterparts is a consequence of the hydration of these CSCs [28–30]. Carbonation of  $\text{Ca}(\text{OH})_2$  should also be considered as it is inevitable in both clinical and experimental conditions but consistent in all specimens [31].

During the hydration process, calcium silicate hydrates (CSH) are also formed but due to their amorphous structure this phase was not detected with XRD analysis [27, 29, 30]. EDX analysis of the amorphous structures identified in SEM evaluations revealed the presence of Ca, Si, and O, which are indicative of CSH.

In ProRoot MTA, exposure to blood and acid reduced the peak size of  $\text{Ca}(\text{OH})_2$  compared to specimens exposed to

PBS. These results are consistent with previous studies [20, 26, 32]. Two hypotheses can be attributed to this decrease: (a) prohibition of hydration due to exposure to different environmental conditions or (b) dissolution of  $\text{Ca}(\text{OH})_2$  formed as a consequence of hydration. Considering that the peak size of tricalcium silicate and dicalcium silicate was similar in all exposure conditions and smaller than that of the unhydrated powder, it may be concluded that the second hypothesis is more probable.

In the case of Biodentine, the peak size of  $\text{Ca}(\text{OH})_2$  in specimens exposed to PBS and blood were similar, however, in specimens exposed to acid a smaller peak was seen. Interestingly, the peak size of tricalcium and dicalcium silicate was seen in those exposed to acid was quite similar to the unhydrated powder indicating an impairment in the hydration process. Previous studies have reported that several physical properties of Biodentine were affected by acidic environmental pH [32] but not affected by exposure to blood [33]. This may be explained by the presence of calcium chloride [34, 35] and calcium carbonate that both accelerate the setting process [30] and the presence of higher percentage of amorphous phase in its hydrated form [36], thus making this cement less susceptible to environmental conditions. Further research is required regarding this matter.

In the case of CEM Cement, the peak of  $\text{Ca}(\text{OH})_2$  in specimens exposed to blood and acid was smaller than those exposed to PBS. However, their tricalcium and dicalcium silicate peaks were similar and smaller than those seen in the



unhydrated powder. Hence, it may be concluded that when CEM Cement is exposed to either blood or acidic pH, hydration occurs and  $\text{Ca}(\text{OH})_2$  is produced but is dissolved similar to what happens to ProRoot MTA. These conditions were also seen in Retro MTA.

Ettringite was not detectable in any of the specimens in the current study although trace amounts of Al were detected in EDX analysis of ProRoot MTA, CEM Cement, and Retro MTA. This may be due to either formation of small amounts of this phase [26] or limited detection due to dilution as a consequence of grinding the specimens [20]. The absence of ettringite peaks in the hydrated form of Biodentine was predictable as this cement lacks aluminate in its powder [30]. The reduction/absence of the aluminate phase is an added benefit with respect to the workability of the fresh cement paste [30], associated with biological improvements [37], e.g., avoiding the undesirable effects of aluminum (e.g., risks of Parkinson's and Alzheimer's disease) [38] and avoiding the leaching of this trace elements into the surrounding tissues [39, 40].

## Conclusion

Blood or acidic pH exposure resulted in reduction in  $\text{Ca}(\text{OH})_2$  in ProRoot MTA, Retro MTA, and CEM Cement. Blood did not affect the hydration of Biodentine, whereas, acidic pH interfered with its hydration.

**Funding information** The work was supported by Tehran University of Medical Sciences, Tehran, Iran (grant no. 27183).

## Compliance with ethical standards

**Conflict of interest** The authors declare that they have no conflict of interest.

**Ethical approval** This article does not contain any studies with human participants or animals performed by any of the authors.

**Informed consent** For this type of study, formal consent is not required.

## References

- Nekoofar MH, Davies TE, Stone D, Basturk FB, Dummer PM (2011) Microstructure and chemical analysis of blood-contaminated mineral trioxide aggregate. *Int Endod J* 44:1011–1018. <https://doi.org/10.1111/j.1365-2591.2011.01909.x>
- Marconyak LJ Jr, Kirkpatrick TC, Roberts HW, Roberts MD, Aparicio A, Himel VT, Sabey KA (2016) A comparison of coronal tooth discoloration elicited by various endodontic reparative materials. *J Endod* 42(3):470–473. <https://doi.org/10.1016/j.joen.2015.10.013>
- Kohli MR, Yamaguchi M, Setzer FC, Karabucak B (2015) Spectrophotometric analysis of coronal tooth discoloration induced by various bioceramic cements and other endodontic materials. *J Endod* 41(11):1862–1866. <https://doi.org/10.1016/j.joen.2015.07.003>
- Nosrat A, Nekoofar MH, Bolhari B, Dummer PM (2012) Unintentional extrusion of mineral trioxide aggregate: a report of three cases. *Int Endod J* 45(12):1165–1176. <https://doi.org/10.1111/j.1365-2591.2012.02082.x>
- Bakhtiar H, Nekoofar MH, Aminishakib P, Abedi F, Naghi Moosavi F, Esnaashari E, Azizi A, Esmailian S, Ellini MR, Mesgarzadeh V, Sezavar M, About I (2017) Human pulp responses to partial pulpotomy treatment with TheraCal as compared with Biodentine and ProRoot MTA: a clinical trial. *J Endod* 43:1786–1791. <https://doi.org/10.1016/j.joen.2017.06.025>
- Butt N, Talwar S, Chaudhry S, Nawal RR, Yadav S, Bali A (2014) Comparison of physical and mechanical properties of mineral trioxide aggregate and Biodentine. *Indian J Dent Res* 25(6):692–697. <https://doi.org/10.4103/0970-9290.152163>
- Kim JR, Nosrat A, Fouad AF (2015) Interfacial characteristics of Biodentine and MTA with dentine in simulated body fluid. *J Dent* 43(2):241–247. <https://doi.org/10.1016/j.jdent.2014.11.004>
- Setbon HM, Devaux J, Iserentant A, Leloup G, Leprince JG (2014) Influence of composition on setting kinetics of new injectable and/or fast setting tricalcium silicate cements. *Dent Mater* 30(12):1291–1303. <https://doi.org/10.1016/j.dental.2014.09.005>
- Camilleri J, Laurent P, About I (2014) Hydration of Biodentine, TheraCal LC, and a prototype tricalcium silicate-based dentin replacement material after pulp capping in entire tooth cultures. *J Endod* 40(11):1846–1854. <https://doi.org/10.1016/j.joen.2014.06.018>
- Esmaili B, Alaghehmand H, Kordafshari T, Daryakenari G, Ehsani M, Bijani A (2016) Coronal discoloration induced by calcium-enriched mixture, mineral trioxide aggregate and calcium hydroxide: a spectrophotometric analysis. *Iran Endod J* 11(1):23–28. <https://doi.org/10.7508/iej.2016.01.005>
- Shokouhinejad N, Nekoofar MH, Pirmoazen S, Shamshiri AR, Dummer PM (2016) Evaluation and comparison of occurrence of tooth discoloration after the application of various calcium silicate-based cements: an ex vivo study. *J Endod* 42(1):140–144. <https://doi.org/10.1016/j.joen.2015.08.034>
- Rouhani A, Akbari M, Farhadi-Faz A (2016) Comparison of tooth discoloration induced by calcium-enriched mixture and mineral trioxide aggregate. *Iran Endod J* 11(3):175–178. <https://doi.org/10.7508/iej.2016.03.005>
- Utneja S, Nawal RR, Talwar S, Verma M (2015) Current perspectives of bio-ceramic technology in endodontics: calcium enriched mixture cement—review of its composition, properties and applications. *Restor Dent Endod* 40(1):1–13. <https://doi.org/10.5395/rde.2015.40.1.1>
- Kang SH, Shin YS, Lee HS, Kim SO, Shin Y, Jung IY, Song JS (2015) Color changes of teeth after treatment with various mineral trioxide aggregate-based materials: an ex vivo study. *J Endod* 41(5):737–741. <https://doi.org/10.1016/j.joen.2015.01.019>
- Ha WN, Bentz DP, Kahler B, Walsh LJ (2015) D90: the strongest contributor to setting time in mineral trioxide aggregate and Portland cement. *J Endod* 41(7):1146–1150. <https://doi.org/10.1016/j.joen.2015.02.033>
- Malkondu O, Karapinar Kazandag M, Kazazoglu E (2014) A review on biodentine, a contemporary dentine replacement and repair material. *Biomed Res Int* 2014:160951. <https://doi.org/10.1155/2014/160951>
- Bakhtiar H, Mirzaei H, Bagheri MR, Fani N, Mashhadiabbas F, Baghaban Eslaminejad M, Sharifi D, Nekoofar MH, Dummer P (2017) Histologic tissue response to furcation perforation repair using mineral trioxide aggregate or dental pulp stem cells loaded onto treated dentin matrix or tricalcium phosphate. *Clin Oral Investig* 21:1579–1588. <https://doi.org/10.1007/s00784-016-1967-0>
- Nekoofar MH, Stone DF, Dummer PM (2010) The effect of blood contamination on the compressive strength and surface

- microstructure of mineral trioxide aggregate. *Int Endod J* 43(9): 782–791. <https://doi.org/10.1111/j.1365-2591.2010.01745.x>
19. Bolhari B, Nekoofar MH, Sharifian M, Ghabrai S, Meraji N, Dummer PM (2014) Acid and microhardness of mineral trioxide aggregate and mineral trioxide aggregate-like materials. *J Endod* 40(3):432–435. <https://doi.org/10.1016/j.joen.2013.10.014>
  20. Nekoofar MH, Davies TE, Stone D, Basturk FB, Dummer PM (2011) Microstructure and chemical analysis of blood-contaminated mineral trioxide aggregate. *Int Endod J* 44(11): 1011–1018. <https://doi.org/10.1111/j.1365-2591.2011.01909.x>
  21. Sheykhrezae MS, Meraji N, Ghanbari F, Nekoofar MH, Bolhari B, Dummer PMH (2017) Effect of blood contamination on the compressive strength of three calcium silicate-based cements. *Aust Endod J*. <https://doi.org/10.1111/aej.12227>
  22. Provenzano JC, Rocas IN, Tavares LF, Neves BC, Siqueira JF Jr (2015) Short-chain fatty acids in infected root canals of teeth with apical periodontitis before and after treatment. *J Endod* 41(6):831–835. <https://doi.org/10.1016/j.joen.2015.02.006>
  23. Nekoofar M, Aseeley Z, Dummer P (2010) The effect of various mixing techniques on the surface microhardness of mineral trioxide aggregate. *Int Endod J* 43(4):312–320
  24. Namazikhah MS, Nekoofar MH, Sheykhrezae MS, Salariyeh S, Hayes SJ, Bryant ST, Mohammadi MM, Dummer PM (2008) The effect of pH on surface hardness and microstructure of mineral trioxide aggregate. *Int Endod J* 41:108–116. <https://doi.org/10.1111/j.1365-2591.2007.01325.x>
  25. Marques MR, Loebenberg R, Almukainzi M (2011) Simulated biological fluids with possible application in dissolution testing. *Dissolut Technol* 18(3):15–28. <https://doi.org/10.14227/DT180311P15>
  26. Lee YL, Lee BS, Lin FH, Yun Lin A, Lan WH, Lin CP (2004) Effects of physiological environments on the hydration behavior of mineral trioxide aggregate. *Biomaterials* 25(5):787–793
  27. Grazziotin-Soares R, Nekoofar MH, Davies TE, Bafail A, Alhaddar E, Hubler R, Busato AL, Dummer PM (2014) Effect of bismuth oxide on white mineral trioxide aggregate: chemical characterization and physical properties. *Int Endod J* 47:520–533. <https://doi.org/10.1111/iej.12181>
  28. Camilleri J (2010) Hydration characteristics of calcium silicate cements with alternative radiopacifiers used as root-end filling materials. *J Endod* 36(3):502–508. <https://doi.org/10.1016/j.joen.2009.10.018>
  29. Basturk FB, Nekoofar MH, Gunday M, Dummer PMH (2017) X-ray diffraction analysis of MTA mixed and placed with various techniques. *Clin Oral Investig*. <https://doi.org/10.1007/s00784-017-2241-9>
  30. Camilleri J, Sorrentino F, Damidot D (2013) Investigation of the hydration and bioactivity of radiopacified tricalcium silicate cement, Biodentine and MTA Angelus. *Dent Mater* 29(5):580–593. <https://doi.org/10.1016/j.dental.2013.03.007>
  31. Lee YL, Wang WH, Lin FH, Lin CP (2017) Hydration behaviors of calcium silicate-based biomaterials. *J Formos Med Assoc* 116(6): 424–431. <https://doi.org/10.1016/j.jfma.2016.07.009>
  32. Kayahan MB, Nekoofar MH, McCann A, Sunay H, Kaptan RF, Meraji N, Dummer PM (2013) Effect of acid etching procedures on the compressive strength of 4 calcium silicate-based endodontic cements. *J Endod* 39:1646–1648. <https://doi.org/10.1016/j.joen.2013.09.008>
  33. Bolhari B, Ashofteh Yazdi K, Sharifi F, Pirmoazen S (2015) Comparative scanning electron microscopic study of the marginal adaptation of four root-end filling materials in presence and absence of blood. *J Dent (Tehran)* 12(3):226–234
  34. Grech L, Mallia B, Camilleri J (2013) Characterization of set intermediate restorative material, biodentine, bioaggregate and a prototype calcium silicate cement for use as root-end filling materials. *Int Endod J* 46(7):632–641. <https://doi.org/10.1111/iej.12039>
  35. Formosa LM, Mallia B, Camilleri J (2012) The effect of curing conditions on the physical properties of tricalcium silicate cement for use as a dental biomaterial. *Int Endod J* 45(4):326–336. <https://doi.org/10.1111/j.1365-2591.2011.01980.x>
  36. Grazziotin-Soares R, Nekoofar MH, Davies T, Hubler R, Meraji N, Dummer PMH (2017) Crystalline phases involved in the hydration of calcium silicate-based cements: semi-quantitative Rietveld X-ray diffraction analysis. *Aust Endod J*. <https://doi.org/10.1111/aej.12226>
  37. De-Deus G, Canabarro A, Alves G, Linhares A, Senne MI, Granjeiro JM (2009) Optimal cytocompatibility of a bioceramic nanoparticulate cement in primary human mesenchymal cells. *J Endod* 35(10):1387–1390. <https://doi.org/10.1016/j.joen.2009.06.022>
  38. Forbes WF, Gentleman JF (1998) Risk factors, causality, and policy initiatives: the case of aluminum and mental impairment. *Exp Gerontol* 33(1–2):141–154
  39. Camilleri J, Kralj P, Veber M, Sinagra E (2012) Characterization and analyses of acid-extractable and leached trace elements in dental cements. *Int Endod J* 45(8):737–743. <https://doi.org/10.1111/j.1365-2591.2012.02027.x>
  40. Basturk FB, Nekoofar MH, Gunday M, Dummer PM (2014) Effect of various mixing and placement techniques on the flexural strength and porosity of mineral trioxide aggregate. *J Endod* 40:441–445. <https://doi.org/10.1016/j.joen.2013.08.010>